2020

Evaluation of an Ag85B Immunosensor with Potential for Electrochemical Mycobacterium Tuberculosis Diagnostics

Brian Murphy

Eithne Dempsey

The Electrochemical Society
Advancing solid state & electrochemical science & technology

Evaluation of an Ag85B immunosensor with potential for electrochemical Mycobacterium tuberculosis diagnostics

Evaluation of an Ag85B immunosensor with potential for electrochemical Mycobacterium tuberculosis diagnostics

SCHOLARONE™
Manuscripts

Evaluation of an Ag85B Immunosensor with Potential for Electrochemical *Mycobacterium tuberculosis* Diagnostics

Brian Murphy[1] and Eithne Dempsey[2,z]

[1]Centre of Applied Science for Health (CASH), Technological University Dublin (TU Dublin)- Tallaght Campus, Dublin 24, Ireland

[2]Department of Chemistry, Kathleen Lonsdale Institute for Human Health Research, Maynooth University, Maynooth Co. Kildare, Ireland

[z]E-mail: eithne.dempsey@mu.ie

Abstract

Tuberculosis remains a major global health concern, especially in the developing world, and monitoring/early detection of the disease relies on low cost technologies that provide rapid and accurate results. *Mycobacterium tuberculosis* is the responsible bacterial pathogen and it is currently estimated by the World Health Organisation (WHO), that one quarter of the world's population, mainly in the developing world, is infected with TB. The overall aim of this work was to advance a screening electrochemical sensor for label free detection of Ag85B, a member of the Antigen 85 complex - major secretary protein of *M. Tuberculosis* and biomarker for disease. An indirect ELISA Ag85B assay was optimised with capture antibody and antigen levels determined via a checkerboard titration (0.625µg.ml^{-1} and 2.5 µg.ml^{-1} respectively). Following assay development, crosslinking of the bioreceptor Anti-Ag85B onto electrochemically deposited gold nanoparticle (AuNP) modified carbon electrodes was achieved and Ag85B binding successfully evaluated electrochemically via cyclic voltammetry. Following each modification step, ΔE_p of a redox probe was monitored and overall results show that GCE/AuNP/anti-Ag85B electrochemical transducers are a viable method for Ag85B detection, capable of measuring antigen levels < 2.5 µg.mL^{-1}.

This paper is part of the JSS Focus Issue on Solid-State Materials and Devices for Biological and Medical Applications.

1

Introduction

TB is a major global threat and according to the WHO approximately 1.7 million annual deaths are attributed to TB [1] with the disease being most prevalent in Asia (58%) and the African region (28%). TB is transmitted from person to person through the air and signs and symptoms of pulmonary TB include a fever, chronic coughing, weight loss and haemoptysis (coughing up blood) [2]. Emergence of multi-drug resistant strains and co-infections with human immunodeficiency (HIV) make for high prevalence and early diagnosis is key for disease control. Importantly, TB can exist both as an active and latent disease and the *Mycobacterium tuberculosis* life cycle can be separated into three main stages, latent, reactivating and active TB. Active TB is responsible for the symptoms mentioned above while patients suffering latent TB show no signs or symptoms of the disease but are at risk of developing the active form of the disease [3]. In order to treat an infection effectively it is paramount that accurate and timely diagnosis is performed, preferably at the point of care (POC). In high-burden, resource-limited countries sputum smear microscopy is used as a primary tool provided there are suitable facilities and a trained microscopist on site with the need for patients to make several visits for accurate diagnosis. The WHO reports that in high-burden countries a significant number of patients fail to return to collect their smear microscopy results. Xpert MTB/RIF has been reviewed as a rapid test concluding the urgent need for new diagnostic strategies [4,5] and development of POC technologies that should allow for rapid diagnosis of a patient at the point where they present themselves, thus allowing for treatment to be delivered in a timely and effective way.

The use of antibodies in TB detection have been considered in the development of a POC diagnostic tool and there have been numerous serological tests (Rapid-kit test and ELISA based test) methods developed as POC diagnostic tools [6,7]. International standards for TB have discouraged the use of serological tests as they have been deemed to be inaccurate and inconsistent [8]. The limitations experienced in antibody detection methods have led to the development of antigen based detection methods. Urine lipoarabinomannan (LAM) antigen has been the first and only commercially available antigen detection assay to date. The Alere Determine TB-LAM kit POC diagnostic tool was evaluated recently by Sahle *et al* in relation to its sensitivity when used in patients with HIV co-infection [9].

2

It is evident that there is an ever-growing need to contribute to further on-site diagnostic tools based on a range of biomarkers – all of which can contribute to TB screening and diagnostics. Antigen 85 complex is the most abundant secretary protein of *M. tuberculosis*. The complex consists of three major proteins, Ag85A (32 kDA), Ag85B (30 kDA) and Ag85C (32.5 kDA). Of these three proteins present in the complex, Ag85B is the most abundant protein [10]. Ag85A, Ag85B and Ag85C are mycolyl -transferases (family of proteins), which are responsible for the synthesis of cell wall components *in M. tuberculosis*. These proteins belong to the CMN (*Corynebacterium*, *Mycobacterium* and *Norcardia*) genera. The cell walls, of organisms present in the CMN genera are comprised of interconnected peptidoglycan and polysaccharide-mycolate complex and are characterised by mycolic acid present on the surface of the cell wall. Mycolic acids are long chain fatty acids that are present in the cell wall envelope and are responsible for pathogenesis and survival of the organism in a host cell. The *Mycobacterium* cell envelope contains mycolic acid comprising of ~60-90 carbons [11]. A study by Zhang *et al* examined new biomarkers including Ag85B in the serodiagnosis between active and latent TB infection, concluding that a combined test of multiple *M. Tuberculosis* secreted proteins may be used as screening antigens for active TB for early diagnosis or screening of h risk population [1]. Other studies have confirmed the presence of the Ag85 complex in the serum of patients, offering a trustworthy TB diagnosis without false positives of other non-TB diseases [12].

The focus of this work was to establish (for the first time) the feasibility of an electrochemical assay for Ag85B based on immunoassay development followed by antibody-antigen binding studies with the aid of cyclic voltammetry. While immunoassays are a fundamental tool for clinical analysis, they require the need for highly skilled specialised staff and the use of desktop equipment in a laboratory setting for generation of optimum results. However, in most remote areas where critical analysis is crucial, often analysis cannot be performed due to the lack of trained personnel or suitable facilities. The development of miniaturised analytical devices such as immunosensors can overcome the need for skilled personnel and use of expensive laboratory equipment. Electrochemical immunosensors are of particular interest due to their high sensitivity, low cost, miniaturisation and simplicity during fabrication [13]. Wang *et al.* described the detection of LAM antibody for the determination of TB. Detection was performed at disposable screen printed electrodes using

3

AuNPs labelled staphylococcal protein (Au-SPA) as an electrochemical tag for detection of LAM antibody (anti-LAM). The immunosensor under optimal conditions obtained a linear concentration response to anti-LAM from 15.6 to 1000 ng.ml^{-1} with a detection limit of 5.3 ng.ml^{-1} [14]. Dionani *et al* examined an ESAT-6 immunoelectrochemical biosensor for TB with the aid of square wave voltammetry and $[Fe(CN)_6{}^{3-}]$ as redox probe [15] with detection limit 7 mg mL^{-1}. Liu *et al.* developed an immunosensor for detection of *Mycobacterium* DNA in sputum samples. The sensor consisted of a glassy carbon electrode (GCE) modified with reduced graphene oxide-gold nanoparticles (rGO-AuNPs) to act as a sensing platform. Gold nanoparticle-polyaniline composites (Au-PANI) were used as tracer label for amplification for the detection of *Mycobacterium* DNA [16].

In order to address the lack of electrochemical immunosensing approaches based on the promising Ag85 protein complex, and to advance electroanalytical screening tools based on suitable TB biomarker measurement we present   (a) indirect ELISA immunoassay development for Ag85B and (b) a preliminary assessment of the use of voltammetry as an electrochemical screening tool for the presence of Ag85B with facile format making it suitable for use at the point of care.

Materials and Methods

Potassium ferricyanide (K$_3$Fe(CN)$_6$), potassium ferrocyanide (K$_4$Fe(CN)$_6$), gold (III) chloride trihydrate (HAuCl$_4$.3H$_2$O, ≥99% purity), 1-Ethyl-3-(3-dimethylaminopropyl)carbodiimide, methiopropamine (MPA), N-Hydroxysuccinimide (NHS), phosphate buffered saline (PBS 0.01 M phosphate buffer, 0.0027 M potassium chloride and 0.137 M sodium chloride, pH 7.4) and PBS with Tween-20 (PBST), anhydrous sodium carbonate, bovine serum albumin (BSA ≥ 96%), 3,3',5,5'-tetramethylbenzidine (TMB liquid substrate for ELISA) were used as received from Sigma Aldrich. Recombinant *Mycobacterium tuberculosis* Ag85B protein, Antigen 85B (ab83471 – 50 μg), rabbit polyclonal to *Mycobacterium tuberculos*is (ab43019 – 100 μl) and Goat Anti-Rabbit IgG H&L (HRP- ab97051-1mg) were purchased from Abcam and used as supplied.

Instrumentation

All electrochemical synthesis and measurements were performed via the use of CH Instruments Inc. CH660C electrochemical potentiostat. A three electrode system was used consisting of a working electrode, glassy carbon electrode (GCE), an Ag/AgCl reference

4

electrode and a platinum wire counter electrode. UV-Visible analysis for optical ELISA measurements was performed on a BioTek Synergy H1 Hybrid plate reader.

Procedures

Checkerboard Titration

A checkerboard titration was performed to determine the optimum concentration for Anti-Ag85B [17] Initially, 50 μl of carbonate coating buffer (pH 9.6) was added to each microwell from column 2 to 12 of the plate. Serial dilution of Ag85B was performed by adding 100 μl of stock Ag85B (10 μg.ml^{-1}) to each microwell of column 1 (Figure 1 A). A 2-fold dilution of Ag85B was performed by dispensing 50 μl from each well of column 1 into each well of column 2. The antigen solution in column 2 was then mixed with carbonate buffer present from the initial coating step by drawing the solution in and out of the multichannel pipette (x5) to ensure adequate mixing. This transfer and mixing process continued from column 2 until column 11. After mixing of the solution in column 11, 50 μl of the solution was dispensed into waste with column 12 only receiving coating buffer, thus acting as a control line as no Ag85B is present in column 12. Antigen concentrations from column 1 to 11 were 10, 5, 2.5, 1.25, 0.63, 0.32, 0.16, 0.08, 0.04, 0.02 and 0.01 μg.ml^{-1} respectively.

The Ag85B coated plate was then wrapped in foil and incubated at 37°C for 1 hr. in a heated oven. The plate was then removed, emptied and vigorously washed 3 times with PBST and air dried before blocking the plate. Blocking of unoccupied sites of the plate was performed by dispensing 100 μl of 1% BSA in PBST to each well and incubating at 37°C for 1 hr. The plate was removed once more and washed using PBST and left to air dry for further use.

Serial dilution for Anti-Ag85B was performed by adding 100 μl of stock Anti-Ag85B (10 μg.ml^{-1}) to all microwells of row A on the plate (Figure 1 B). 50 μl of 1% BSA-PBST was added to the remaining row, B to H. A 2-fold dilution of Anti-Ag85B was performed by dispensing 50 μl of Anti-Ag85B from each well of row A into each well of row B. The antibody solution in row B was then mixed with 1% BSA-PBST present in row B by drawing the solution in and out of the multichannel pipette (x5) to ensure adequate mixing. This transfer and mixing process continued from row B to row G. After the final transfer and mixing process in row G, 50 μl of the solution was removed and dispensed into waste with row H only receiving 1% BSA-PBST, thus acting as a control line as no Anti-Ag85B is

5

present in row H. Antibody dilutions from row A to H were 1/100, 1/200, 1/400, 1/800, 1/1600, 1/3200, 1/6400 and 0 respectively.

The Anti-Ag85B coated plate was foil wrapped and incubated at 37°C for 1 hr. after which it was vigorously washed 3 times with PBST. 100 μl of Goat-rabbit IgG HRP-labelled conjugate (0.1 μg.ml^{-1}) was added to each microwell of the plate and incubated for 1 hr. at 37°C. The plate was removed and washed a further 3 times using PBST before 100 μl of TMB was added to each well and incubated for 15 minutes at room temperature. The enzyme reaction was quenched by the addition of 100 μl of 1 M HCl to each well of the plate, which prevents colour saturation and changes the reaction colour from blue to yellow. The optical density was then measured at 450 nm.

Scheme 1 shows the overall ELISA format employed. The Anti-Ag85B coated plate was foil wrapped and incubated at 37°C for 1 hr. after which it was vigorously washed 3 times with PBST. 100 μl of Goat-rabbit IgG HRP-labelled conjugate (0.1 μg.ml^{-1}) was added to each microwell of the plate and incubated for 1 hr. at 37°C. The plate was removed and washed a further 3 times using PBST before 100 μl of TMB was added to each well and incubated for 15 minutes at room temperature. The enzyme reaction was quenched by the addition of 100 μl of 1 M HCl to each well of the plate, which prevents colour saturation and changes the reaction colour from blue to yellow. The optical density was then measured at 450 nm.

Development of nano gold modified electrode Immunosensor

Prior to AuNP deposition, a GCE electrode was vigorously polished in alumina slurry (1.0, 0.3 and 0.05 µm) followed by continuous cycling in 0.5 M H$_2$SO$_4$ until reproducible currents were observed. The electrode was placed in a three-electrode cell containing a solution of 2.5 mM HAuCl$_4$.3H$_2$O in 0.1 M NaNO$_3$ and cycled over the potential window 0.0 V to +1.0 V for a total of 10 cycles [18]. The electrode was then vigorously rinsed with deionised water to remove any remaining precursor ions. The electrode was labelled GCE/AuNP. The GCE/AuNPs was then immersed in an aqueous 0.01 MPA solution overnight and washed with deionised water to remove any remaining MPA solution. Activation of the carboxylic groups of the thiol linker, now present on the surface of the AuNPs was performed by immersing the modified electrode for 2 hours in an ethanolic solution of 0.01 M EDC/0.01 M NHS (Scheme 2) based on a previously reported approach by our group [18].

6

Detection of Ag85B

Detection of Ag85B was performed at the GCE/AuNP modified electrode. 5 µl of Anti-Ag85B (0.625 µg.ml^{-1}) was dispensed onto the surface of the GCE/AuNP and incubated at 37°C for 1 hr. after which the GCE/AuNP was rinsed with deionised water to remove any excess Anti-Ag85B. The GCE/AuNP/Anti-Ag85B was then dried under argon gas. 5 µl of 1% BSA-PBST was then dispensed onto the surface of the GCE/AuNP/Anti-Ag85B to prevent non-specific binding and incubated for 1 hr. at 37°C. The GCE/AuNP/Anti-Ag85B/BSA was rinsed and dried with argon gas. 5 µl of Ag85B (2.5 µg.ml^{-1}) was then dispensed onto the surface of the GCE/AuNP/AntiAg85B/BSA and incubated for 1 hr. at 37°C. Ag85B binding was then accessed electrochemically using a redox probe.

Results and Discussion

ELISA Development

Checkerboard Titration for Ag85B Indirect ELISA Development

A checkerboard titration (Figure 2) was performed to identify the optimum concentration of Anti-Ag85B for the development of an indirect ELISA assay. A 15-minute enzyme-substrate reaction was performed by reacting Goat-rabbit IgG HRP-labelled conjugate with TMB and the subsequent optical density is measured at 450 nm. A plateau region was expected where little change in optical density is observed due to the fact that different combinations of Ag85B and Anti-Ag85B concentrations decrease across the plate.

An initial 1/100 dilution of Anti-Ag85B (1 mg.ml^{-1}) was carried out yielding a stock concentration of 10 µg.ml^{-1}. The stock Anti-Ag85B (10 µg.ml^{-1}) was then serially diluted from row B to G, yielding concentrations of 5, 2.5, 1.25, 0.63, 0.32 and 0.16 µg.ml^{-1} respectively. **Figure 3-10** illustrates the result for optical densities recorded for Anti-Ag85B in response to Ag85B. At high concentrations of Anti-Ag85 up to 1/400 dilution, saturation of the antibody-antigen system was observed with concentrations of Ag85B less than 2 µg.ml^{-1}. Selection of the optimum antibody concentration was based on which combination of Anti-Ag85B and Ag85B gave 75% of the absorbance plateau [20] Singh et al This was achieved with Anti-Ag85B using a dilution of 1:1600 to give a concentration of 0.625 µg.ml^{-1}.

7

Development of an Ag85B Immunosensor based on AuNPs

Electrochemical deposition of AuNPs at a GCE electrode was performed by cyclic voltammetry. Figure 3 shows a cyclic voltammogram for AuNPs deposition, where Au(III) was reduced to Au(0) at 0.39 V *vs.* Ag/AgCl. The shift in peak position observed after 10 cycles, from 0.39 V to 0.7 V confirmed AuNPs deposition [18].

$$AuCl_4 + 3e^- \rightleftharpoons Au\ (0) + 4Cl^-$$
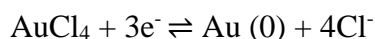
AuNPs characterisation was performed by cycling the GCE/AuNPs in 0.5 M H_2SO_4, to ensure that AuNP deposition was successful. Figure 3 illustrates characteristic features of AuNPs in acid with gold oxide formation and reduction present at 1.3 V and 0.9 V respectively [21,22].

The modification process for the GCE/AuNPs immunosensor was measured by examining the electrode in a solution containing 5 mM $[Fe(CN)_6]^{3-/4-}$ (1:1) redox couple in 0.01 M PBS (pH 7.4) over the range 0.8 V to -0.2 V at a scan rate of 0.1 $V.s^{-1}$. Figure 4 shows the influence of AuNPs deposition on the redox couple. It was observed that oxidation (115.20 μA) and reduction (-110.40 μA) currents increased and a shift in ΔE_p (119.20 mV) occurred. It was expected that AuNPs deposition would result in an increase in current in comparison to bare GCE as nanoparticles provide a high surface to volume ratio thus enhancing the rate of electron transfer [18,23].

Following AuNP deposition the effect of the self-assembled monolayer of MPA was examined. Figure 5 illustrates that MPA inhibits electron transfer of the redox probe as a decrease in peak oxidation (84.69 μA) and reduction currents (-82.81 μA) as well as a large change in ΔE_p (from 119.20 mV to 240 mV) was observed [18]. Immobilisation of Anti-Ag85B onto the surface of the newly formed GCE/AuNPs/MPA was performed by dispensing 5 μl of Anti-Ag85B (0.625 $μg.ml^{-1}$) onto the surface of the GCE/AuNPs/MPA following activation of the carboxylic thiol linker and incubated for 1 hr. at 37°C. The immobilisation of Anti-Ag85B resulted in a decrease in oxidation current (76.43 μA) as well as shifts in ΔE_p (from 240 mV to 265.50 mV) values as seen in Figure 6 suggesting that Anti-Ag85B was successfully immobilised onto the surface of the GCE/AuNPs/MPA resulting in the formation of GCE/AuNPs/MPA/Anti-Ag85B immunosensor.

8

To prevent non-specific binding and to block any remaining active sites 5 µl of 1% BSA-PBST was dispensed onto the surface of the GCE/AuNPs/MPA/Anti-Ag85B and incubated at 37ºC for 1 hr. Figure 7 shows the largest change in ΔE_p (from 265.50 mV to 487 mV) and further decreases in oxidation (60.62 µA) and reduction currents (-64.87 µA) following deposition of 1% BSA-PBST.

Electrochemical detection of Ag85B at GCE/AuNPs/MPA/Anti-Ag85B/BSA was examined by depositing 5 µl of Ag85B (2.5 µg.ml^{-1}) and incubating for 1 hr. at 37ºC. **Figure 8** illustrates the resulting effect of Ag85B on the GCE/AuNPs/MPA/Anti-Ag85B/BSA sensor using a redox probe. A further decrease in oxidation (54.06 µA) and reduction current (-56.88 µA) was observed as well as a shift in ΔE_p (from 487 mV to 499.40 mV) following the introduction of 2.5 µg.ml^{-1} Ag85B. The changes in ΔE_p and peak currents were attributed to Ag85B causing resistance to electron transfer, thus suggesting that significant binding has occurred between Anti-Ag85B and Ag85B.

The results obtained for each modification step of the Ag85B immunosensor are shown in **Table I** They illustrate the change in I_{ox} ,I_{red} and ΔE_p following each modification step of the Ag85B immunosensor as measured via a redox probe.

From Table 1 and Figure 9 it was observed that with each modification step, changes to the oxidation and reduction current peaks and ΔE_p were observed. AuNPs deposition resulted in changes to peak currents and a shift in ΔE_p compared to a bare GCE due to the high surface to volume ratio of the nanoparticles. The self-assembled monolayer of MPA resulted in decrease to peak currents and a large shift in ΔE_p due to MPA inhibiting electron transfer. Immobilisation of Anti-Ag85B to the Ag85B immunosensor was confirmed by further changes to peak currents and shifts in ΔE_p. 5 µl of 1% BSA-PBST was introduced to the sensor to prevent non-specific binding of Anti-Ag85B and resulted in further decrease to peak currents and a large change (as expected) in ΔE_p (222 mV vs Ag/AgCl). Finally, Ag85B binding (2.5 µg.ml^{-1}) was confirmed by observing decreases in peak current and an increase in ΔE_p (13 mV) over that of the BSA effect for n=3 electrodes.

9

The concentration of Ag85B detected by the Ag85B immunosensor in this study was 2.5 μg.ml^{-1}. When referring to the literature, concentrations of Ag85B have been detected ranging from the femtogram (fg) to the μg level. Kim *et al.* developed a sandwich assay for detection of Ag85B using quantum dots and gold nanorods. The sensor had a linear range from 0.013 to 1 ng.ml^{-1} with a limit of detection (LOD) of 0.013 ng.ml^{-1} [24]. Saengdee *et al.* detected Ag85B over the linear range of 0.12 μg.ml^{-1} to 1.0 μg.ml^{-1} [25]. When comparing the Ag85B immunosensor in this study to that of sensors found in the literature the LOD for this sensor is in the upper limits for Ag85B detection at this stage of the work. From further investigations into the literature there appears to be no predetermined physiological concentration for Ag85B in TB patients and it also may be related to clinical sample type.

Table 2 presents a comparison of analytical performance for reported Ag85B assay detection methods and sensors, with respect to current literature. The majority of these approaches are laboratory confined while the immunosensing device proposed in this work has the advantages of providing a portable, low-cost platform for the rapid detection of Ag85B although; further studies to validate analytical performance are required. Additionally, the proposed device has significant novelty due to there being very limited reports of biosensors for Ag85B detection.

Conclusions

The double burden of TB and HIV remains a challenge to medicine and public health in developing countries with disease control dependant on prompt diagnostics and therapeutic intervention. Though further work is required and planned for, the methodology developed for Ag85B and presented here is promising, filling a knowledge gap in relation to its viability as a rapid diagnostic tool. Assay development realised a working ELISA method for Ag85B with optimal levels of bioreagents suitable for transfer onto an electrochemical transducer for the first time. Functionalisation of AuNP and subsequent coupling to anti-Ag85B antibodies realised a simple effective receptor surface with signal discrimination enabled with the assistance of a redox probe. The successful use of AuNPs as a platform for detecting Ag85B will rely on quantitative electrochemical studies which form the next step to evaluate sensitivity and limits of detection. Electrochemical impedance spectroscopy and/or differential pulse voltammetry will play a role in this regard. Further investigations into the

10

fabrication and miniaturisation of an AuNPs based immunosensor for Ag85B detection may be advanced with the aid of screen printed transducers integrated with lateral flow membranes for clinical sample processing, coupled with micro-potentiostat control enabling portable operation and deployment.

Acknowledgements

References

1. C. Zhang X Song, *Y* Zhao, H Zhang, S Zhao, F. Mao, B. Bai, S.C. Wu, C. Hi,. *Mycobacterium tuberculosis* Secreted Proteins As Potential Biomarkers for the Diagnosis of Active Tuberculosis and Latent Tuberculosis Infection, *Journal of Clinical Laboratory Analysis* **29:**375–382 (2015).

2. World Health Organization. *Global Tuberculosis Report* 2015, 20th ed.; World Health Organization: Geneva, 2015. ISBN 9789241565059

3. P. Castan, A. De Pablo, N. Fernández-Romero, J.M. Rubio, B.D. Cobb, J. Mingorance, C. Toro, Point-of-Care System for Detection of Mycobacterium Tuberculosis and Rifampin Resistance in Sputum Samples. *J. Clin. Microbiol.* **52**(2):502–507 (2014).

4. J.D. Donovan, D.D. Thu, N.H. Phu, V.T.M. Dung, Mong, T.P. Quang, H.D.T. Nghia, P.K.H. Oanh, T.B. Nhu, N.V.V. Chau, V.T.N. Ha, V.T.T. Hang, D.H.K. Trinh, R.B. Geskus, L.V. Tan, N.T.T. Thuon, G.E. Thwaites, Xpert MTB/RIF Ultra versus Xpert MTB/RIF for the diagnosis of tuberculous meningitis: a prospective, randomised, diagnostic accuracy study *The Lancet Infectious Diseases* **20**(3): 299-307 (2020).

5. K.R. Steingart, I. Schiller, D.J. Horne, M. Pai, C.C. Boehme, N. Dendukuri Xpert® MTB/RIF Assay for Pulmonary Tuberculosis and Rifampicin Resistance in Adults. *Cochrane Database Syst. Rev.* 1:CD009593 (2014).

6. N.P. Pai, M. Pai,. Point-of-Care Diagnostics for HIV and Tuberculosis: Landscape, Pipeline, and Unmet Needs. *Discov. Med.* **13**(68):35–45 (2012).

7. M. Pai, Improving TB Diagnosis: Difference between Knowing the Path and Walking the Path. *Expert Rev. Mol. Diagn.* **11**(3):241–244 (2011).

8. J .Grenier, L. Pinto, D. Nair, K. Steingart, D. Dowdy, A. Ramsay, M. Pai. Widespread Use of Serological Tests for Tuberculosis: Data from 22 High-Burden Countries. *Eur. Respir. J.* **39**(2):502–505 (2012).

9. S.N. Sahle, D.T. Asress, K.D. Tullu, A.G. Weldemariam, H.H. Tola, Y.A. Awas, G.G. Hagos, M.G. Worku D.K. Misgina, Performance of point-of-care urine test in diagnosing tuberculosis suspects with and without HIV infection in selected peripheral health settings of Addis Ababa, Ethiopia*, BMC Res Notes* **10**:74 (2017).

10. P. Phunpae, S. Chanwong, C. Tayapiwatana, N. Apiratmateekul, A. Makeudom W. Kasinrerk. Rapid Diagnosis of Tuberculosis by Identification of Antigen 85 in Mycobacterial Culture System. *Diagn. Microbiol. Infect. Dis*. **78**(3):242–248 (2014).

11

11. H.G. Ramulu, S. Adindla, l. Guruprasad. Analysis and Modeling of Mycolyl-Transferases in the CMN Group. *Bioinformation* **5**:161–169 (2006).

12. N. Ansari, K. Ghazvini, M. Ramezani, M. Shahdordizadeh, R. Yazdian-Robati, K. Abnous, S.M. Taghdis. Selection of DNA aptamers against Mycobacterium tuberculosis Ag85A, and its application in a graphene oxide-based fluorometric assay *Microchimica Acta* **185**:21-29 (2018).

13. C. Kokkinos, A. Economou, M.I. Prodromidis, Electrochemical Immunosensors: Critical Survey of Different Architectures and Transduction Strategies. *TrAC - Trends Anal. Chem.* **79**:88–105 (2016).

14. L. Wang, C. Leng, S. Tang, J. Lei, H. Ju Enzyme-Free Signal Amplification for Electrochemical Detection of Mycobacterium Lipoarabinomannan Antibody on a Disposable Chip. *Biosens. Bioelectron.* **38**(1):421–424 (2012).

15. M.F. Diouani, O. Ouerghi, A.R.K. Belgacem, C. Tlili, D. Laouini, M. Essafi Detection of ESAT-6 by a label free miniature immuno-electrochemical biosensor as a diagnostic tool for tuberculosis, *Materials Science and Engineering C* **74**: 465–470 (2017).

16. C. Liu, D. Jiang, G. Xiang, L. Liu, F. Liu, X. Pu. An Electrochemical DNA Biosensor for the Detection of *Mycobacterium Tuberculosis*, Based on Signal Amplification of Graphene and a Gold Nanoparticle–Polyaniline Nanocomposite. *Analyst* **139**(21):5460–5465 (2014).

17. Fitzgerald. ELISA Optimization Protocol https://www.fitzgerald-fii.co.uk/media/Protocolsuk/ELISA_Optimization_Protocol.pdf (accessed 22/6/20).

18. A.A. Saeed, B. Singh, M.N. Abbas, Y.M. Issa, E. Dempsey E. Electrocatalytic Nitrite Determination Using Iron Phthalocyanine Modified Gold Nanoparticles. *Electroanalysis* **27**(5):1086–1096 (2015).

19. J. Bart, R. Tiggelaar, M. Yang, S. Schlautmann, H. Zuilhof, H. Gardeniers Room-Temperature Intermediate Layer Bonding for Microfluidic Devices. *Lab Chip* **9**(24):3481 (2009).

20. R.P. Singh, B.P. Sreenivasa, P. Dhar, L.C. Shah, S.K. Bandyopadhyay, Development of a Monoclonal Antibody Based Competitive-ELISA for Detection and Titration of Antibodies to Peste Des Petits Ruminants (PPR) Virus. *Vet. Microbiol.* **98**(1):3–15 (2004).

21. L.D. Burke, P.F. Nugent, The Electrochemistry of Gold: I the Redox Behaviour of the Metal in Aqueous Media. *Gold Bull.* **30** (2):43–53 (1997).

22. K. Caban, A. Offenhäusser, D. Mayer Electrochemical Characterization of the Effect of Gold Nanoparticles on the Electron Transfer of Cytochrome C. *Phys. Status Solidi A* **206**(3): 489–500 (2009).

23. Y. Fu, R. Yuan, D. Tang, Y. Chai, L. Xu Study on the Immobilisation of Anti-IgG on Au-Colloid Modified Gold Electrode via Potentiometric Immunosensor, Cyclic Voltammetry, and Electrochemical Impedance Techniques. *Colloids Surf. B. Biointerfaces* **40**(1):61–66 (2005)

24. E.J. Kim, E.B. Kim, S.W. Lee, S.A. Cheon, H-.J. Kim, J. Lee, M-K. Lee , S. Ko, T.J. Park, An Easy and Sensitive Sandwich Assay for Detection of Mycobacterium Tuberculosis Ag85B Antigen Using Quantum Dots and Gold Nanorods. *Biosens. Bioelectron.* **87**:150–156 (2017).

25. P. Saengdee, W. Chaisriratanakul, W. Bunjongpru, W. Sripumkhai, A. Srisuwan, C. Hruanun, A. Poyai, P. Phunpae, S. Pata,, W.A. Jeamsaksiri Silicon Nitride ISFET

Based Immunosensor for Ag85B Detection of Tuberculosis. *Analyst* **141**(20):5767–5775 (2016).

26. P. Phunpae, S. Chanwong, C. Tayapiwatana, N. Apiratmateekul, A. Makeudom, W. Kasinrerk,. Rapid Diagnosis of Tuberculosis by Identification of Antigen 85 in Mycobacterial Culture System. *Diagn. Microbiol. Infect. Dis*. **78**(3):242–248 (2014).

27. N. Singh, V. Sreenivas, K.B. Gupta, A. Chaudhary, A. Mittal, M. Varma-Basil, R. Prasad, S.K. Gakhar, G.K. Khuller, P.K. Mehta. Diagnosis of Pulmonary and Extrapulmonary Tuberculosis Based on Detection of Mycobacterial Antigen 85B by Immuno-PCR. *Diagn. Microbiol. Infect. Dis*. **83**(4): 359–364 (2015).

13

50μl to waste

S = Ag85B stock solution, 10 μg/ml
B = coating buffer solution

50 μl to Waste

S = Anti-Ag85B stock solution, 10 μg/ml
B = 1% BSA-BPST
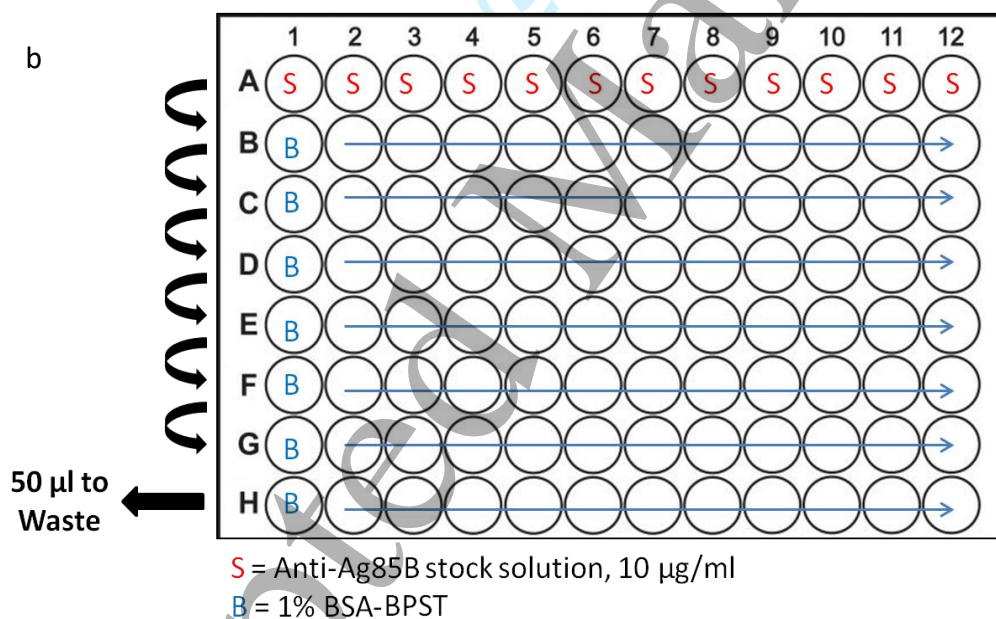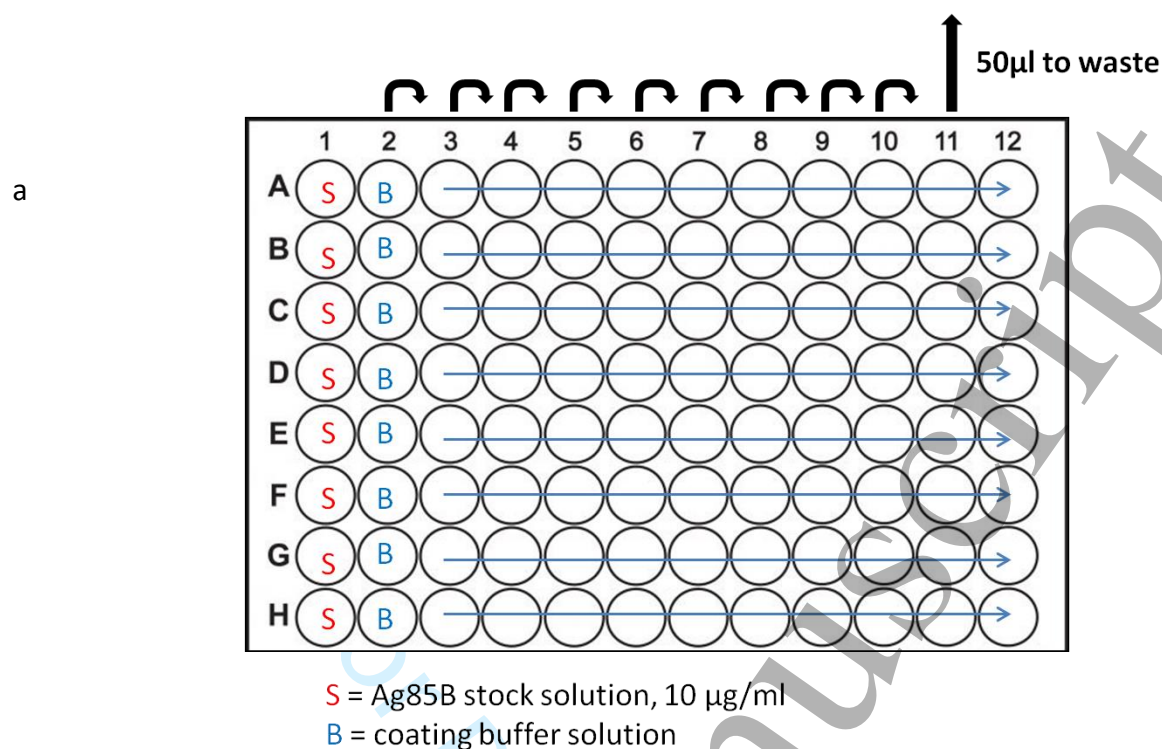
Fig. 1 a Checkerboard titration schematic for serial dilution of antigen Ag85B. Carbonate coating buffer (50 μl) was dispensed in all columns except column 1. Stock Ag85B (10 μg.ml^{-1}) was dispensed into column 1 (100 μL) and serial diluted from column 1 to 11. **b** Checkerboard titration schematic for serial dilution of antibody Ag85B. 1% BSA-PBST (50 μl) was dispensed in all rows except row H. Stock Anti-Ag85B (10 μg.ml^{-1}) was dispensed into row A (100 μL) and serially diluted from row A to G.

14

a.

3,3',5,5'-tetramethylbenzidine → (HRP, H₂O₂) → 3,3',5,5'-tetramethylbenzidine diimine
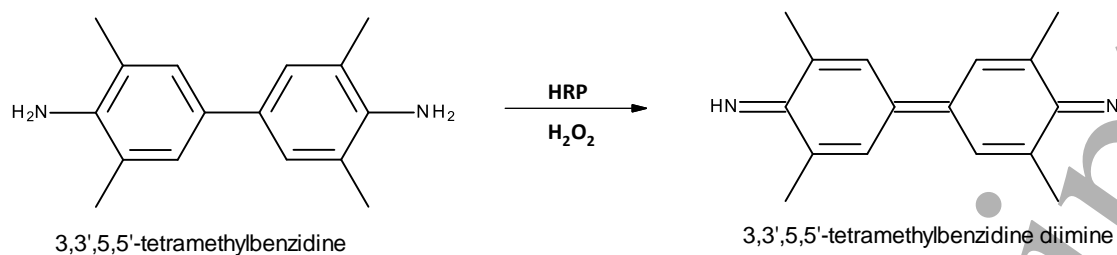
b.
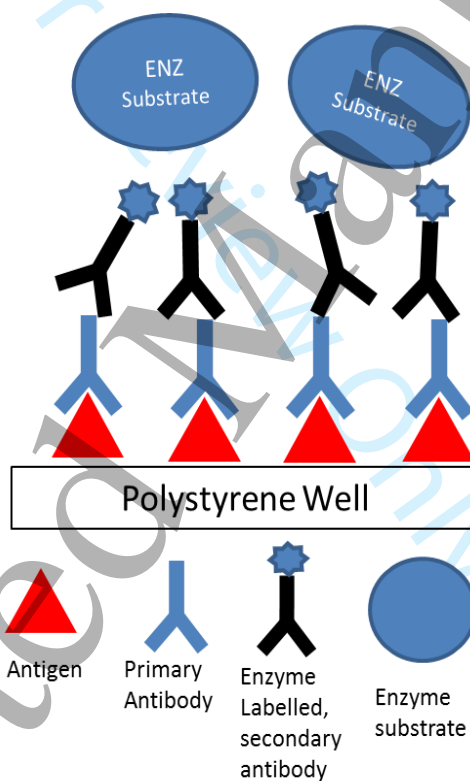
Scheme 1 a. Oxidation of TMB in the presence of H_2O_2 resulting in the formation of 3,3',5,5'-tetramethlybenzidine diimine, which is blue in colour b. schematic representation of indirect ELISA format.

15
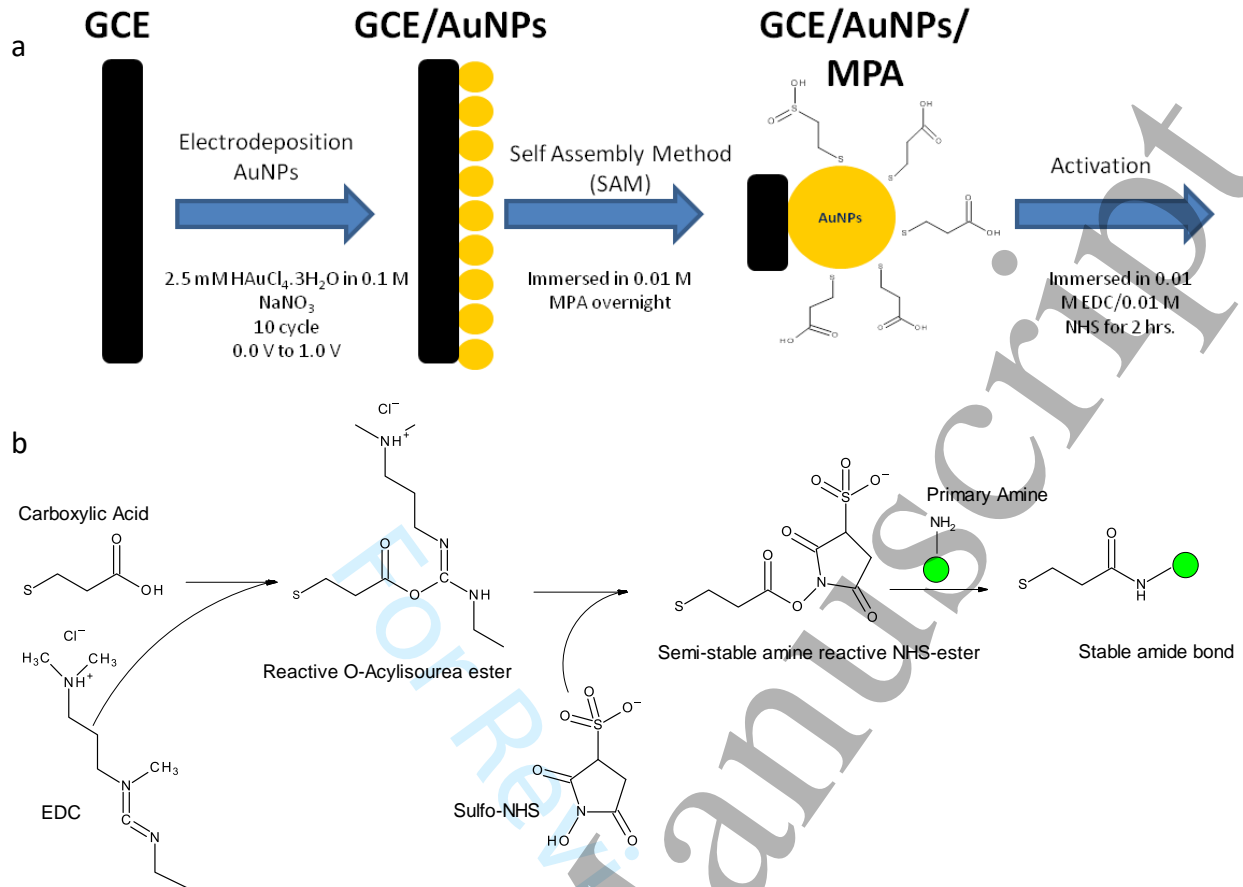
Scheme 2 a. Schematic representation of GCE modification process with AuNPs. b. EDC/NHS coupling reaction scheme to form a stable bond with a primary amine [19].
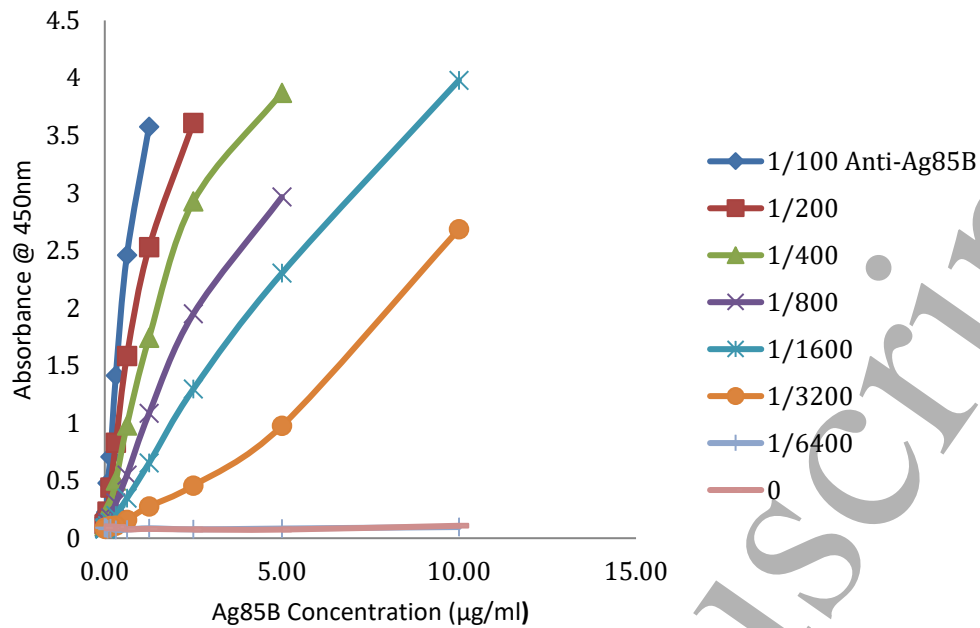
16

Fig. 2 Checkerboard titration plot showing optical density intensity of TMB at 450 nm. Individual data points represent a different combination of Ag85B and Anti-Ag85B concentrations.

17
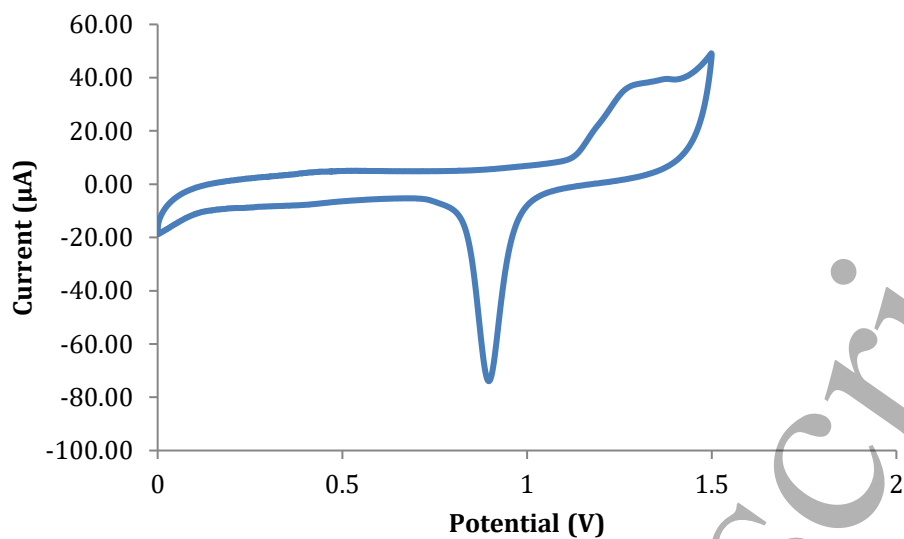
Fig. 3 Cyclic voltammogram for gold nanoparticles with characteristic Au oxide formation (I) at 1.3 V and reduction peak (II) of Au present at 0.9 V vs. Ag/AgCl in 0.5 M H_2SO_4 at GCE, scan rate 0.1 $V.s^{-1}$.

18
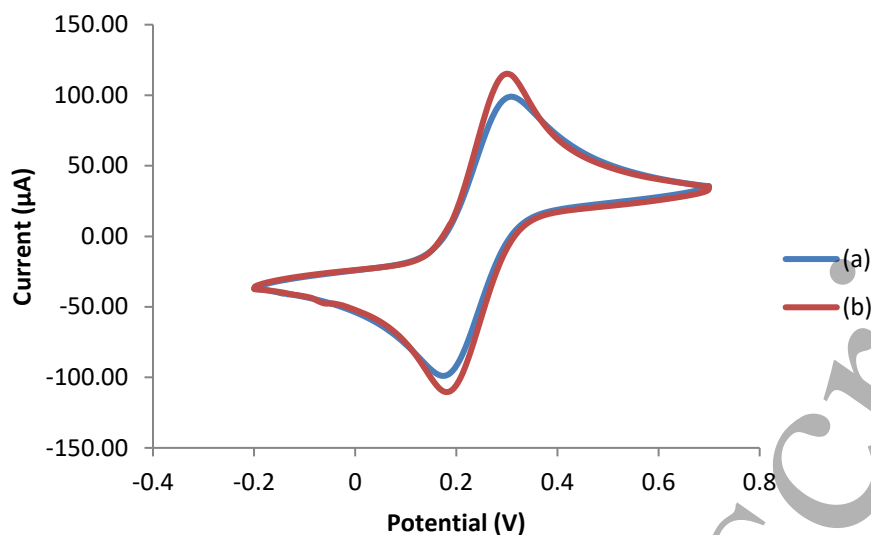
Fig. 4 Cyclic voltammogram of (a) bare GCE and (b) GCE/AuNP in a solution of 5 mM $[Fe(CN)_6]^{3-/4-}$ and 0.01 M PBS (pH 7.4) at scan rate 0.1 $V.s^{-1}$.
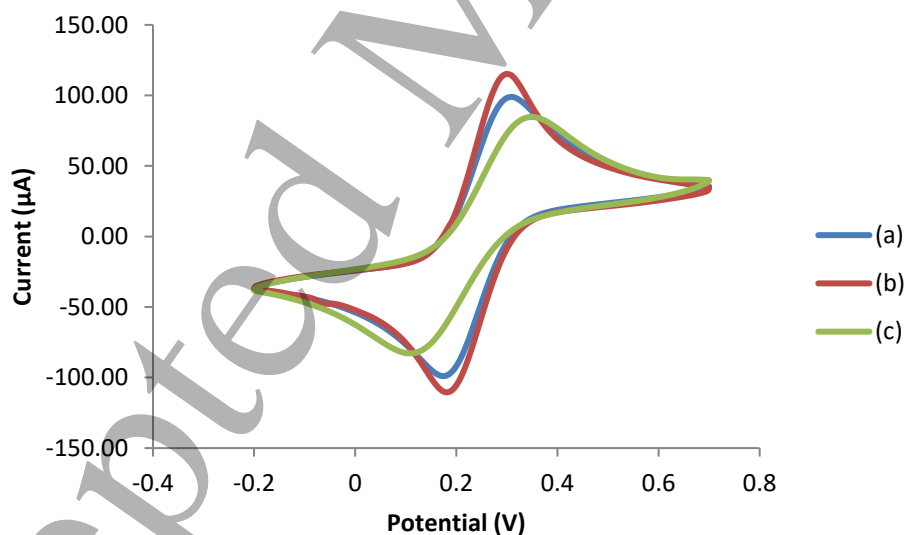
Fig. 5 Cyclic voltammogram of (a) bare GCE, (b) GCE/AuNPs, (c) GCE/AuNPs/MPA in a solution of 5 mM $[Fe(CN)_6]^{3-/4-}$ and 0.01 M PBS (pH 7.4) at scan rate 0.1 $V.s^{-1}$.
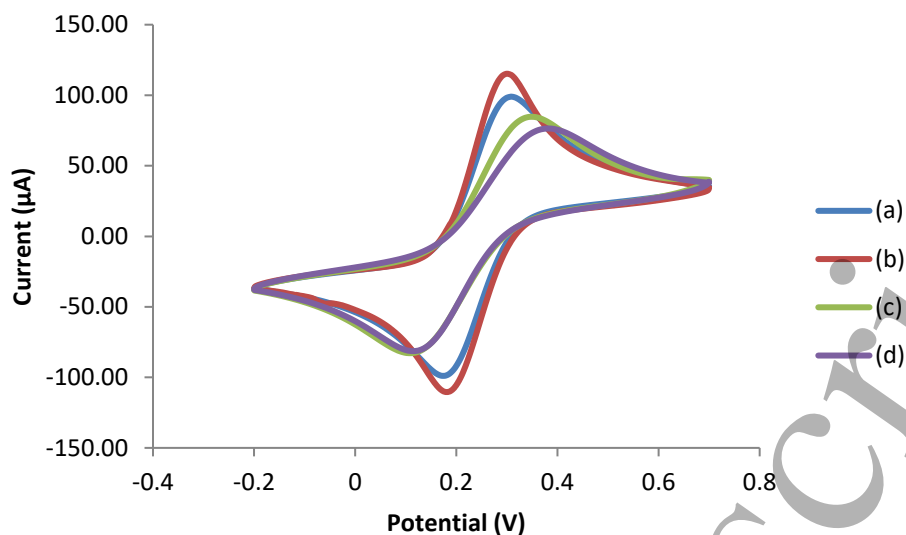
19

Fig. 6 Cyclic voltammogram of (a) bare GCE, (b) GCE/AuNPS, (c) GCE/AuNPs/MPA, (d) GCE/AuNPS/MPA/Anti-Ag85B in a solution of 5 mM $[Fe(CN)_6]^{3-/4-}$ and 0.01 M PBS (pH 7.4) at scan rate 0.1 $V.s^{-1}$.
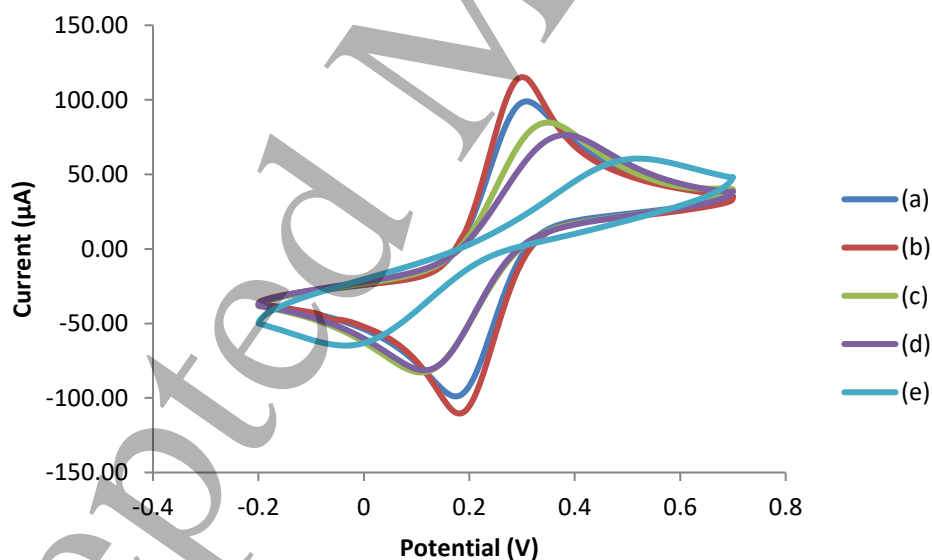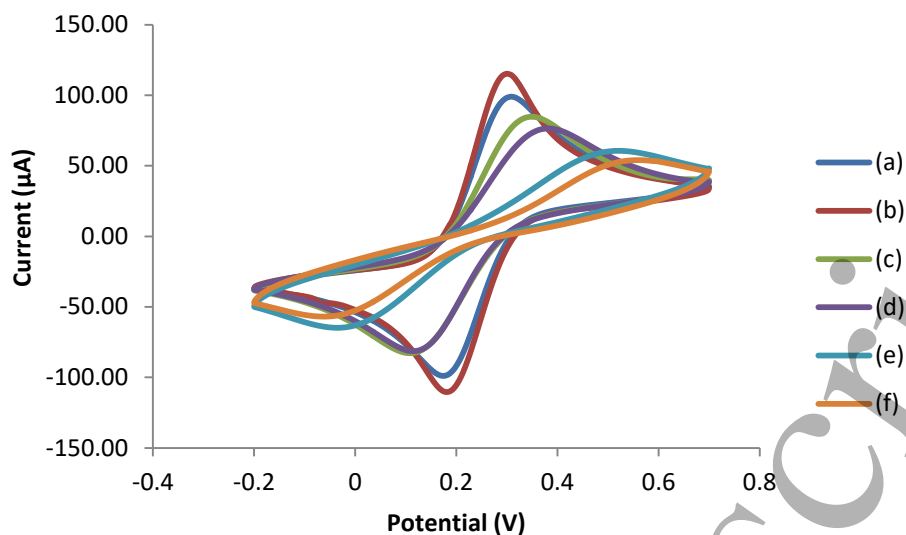

Fig. 7 Cyclic voltammogram of (a) bare GCE, (b) GCE/AuNPS, (c) GCE/AuNPs/MPA, (d) GCE,AuNPS/MPA/Anti-Ag85B, (e) GCE/AuNPS/MPA/Anti-Ag85B/1% BSA in a solution of 5 mM $[Fe(CN)_6]^{3-/4-}$ and 0.01 M PBS (pH 7.4) at scan rate 0.1 $V.s^{-1}$.

20

Fig. 8 Cyclic voltammogram of (a) bare GCE, (b) GCE/AuNPs, (c) GCE/AuNPs/MPA, (d) GCE/AuNPS/MPA/Anti-Ag85B, (e) GCE/AuNPs/MPA/Anti-Ag85B/1% BSA, (f) GCE/AuNPs/MPA/Anti-Ag85B/1% BSA/Ag85B in a solution of 5 mM $[Fe(CN)_6]^{3-/4-}$ and 0.01 M PBS (pH 7.4) at scan rate 0.1 $V.s^{-1}$.

21

Table 1 I_{ox} , I_{red} and ΔE_p values of $[Fe(CN)_6]^{3-/4-}$ redox couple for range of electrode modifications.

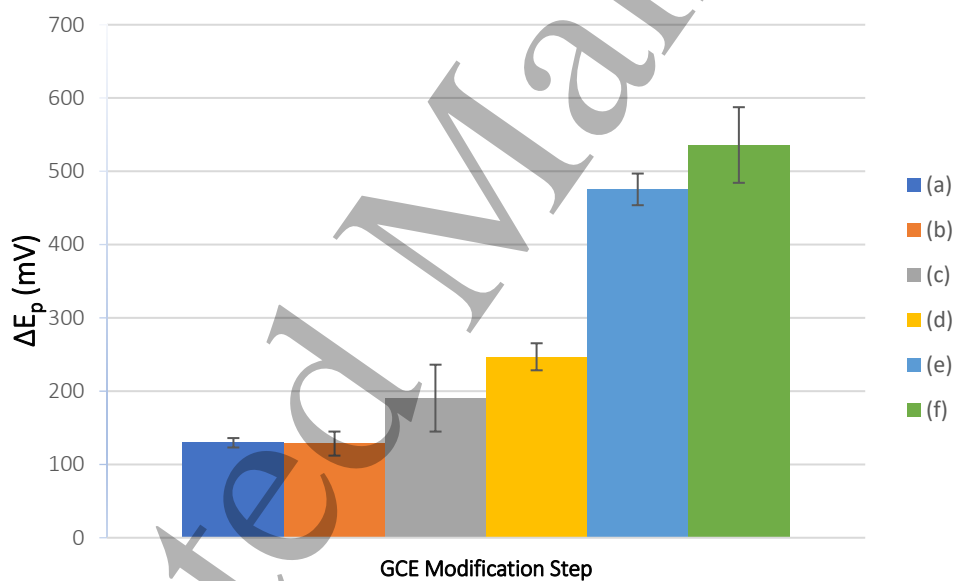| Electrode	I_{ox} (μA)	ΔI_{ox} (μA)	I_{red} (μA)	ΔI_{red} (μA)	ΔE_p(mV)
GCE	99.01	-	-98.86	-	134.50
GCE/AuNPs	115.20	16.19	-110.40	11.54	119.80
GCE/AuNPs/MPA	84.69	30.51	-82.81	27.59	240
GCE/AuNPs/MPA/Anti-Ag85B	76.43	8.26	-81.35	1.46	265.50
GCE/AuNPs/MPA/Anti-Ag85B/BSA	60.62	15.81	-64.87	16.48	487
GCE/AuNPs/MPA/Anti-Ag85B/BSA/Ag85B	54.06	6.56	-56.88	7.99	499.40

Fig. 9 Bar chart illustrating the change in ΔE_p, (a) GCE (b) GCE/AuNPs, (c) GCE/AuNPs/MPA, (d) GCE/AuNPs/MPA/Anti-Ag85B, (e) GCE/AuNPs/MPA/Anti-Ag85B/BSA, (f) GCE/AuNPs/MPA/Anti-Ag85B/BSA/Ag85B where n = 3.

22

Table 2 Comparison of current assays and analytical performance with respect to Ag85B

Antigen	Technique	Electrochemical transduction	Detection range (ng.ml⁻¹)	LOD (ng.ml⁻¹)	Reference
	Sandwich ELISA	-	8-400	8	Phunapae *et al*.[26]
	Indirect ELISA	-	-	10	Singh *et al*. [27]
	Indirect Sandwich ELISA	-	-	1	-
Ag85B	Indirect I-PCR	-	-	0.00001	-
	Indirect sandwich I-PCR	-	-	0.000001	-
	Silicon nitride ISFET	ISFET	120-1000	120	Saengdee *et al*. [25]
	Sandwich ELISA	-	0.013-1	0.013	Kim *et al*. [24]

23